Cu-Graphene water-based hybrid nanofluids: synthesis, stability, thermophysical characterization, and figure of merit analysis

Aabid Hussain Shaik[1] · Samarshi Chakraborty[1] · Shaik Saboor[2] · Kodi Rajesh Kumar[1] · Aaroh Majumdar[1] · Mohammed Rizwan[1] · Müslüm Arıcı[3] · Mohammed Rehaan Chandan[1]

Abstract

Hybrid nanofluids are emerging as an alternative to conventional heat transfer fluids and nanofluids for improving the thermal efficiency of heat exchanging devices synergistically due to their outstanding thermophysical properties associated because of the dispersion of different types of nanoparticles as compared to mono nanofluids. This will help in optimizing fluid characteristics in different flow regimes for several applications. However, enhancing the thermal energy efficiency of heat exchangers is challenging owing to the deprived stability of hybrid nanofluids at greater volume concentrations. This work concentrated on the synthesizing, thermophysical depiction, and thermal performance estimation of stable water-based Cu-graphene hybrid nanofluids using very low volume concentrations of Cu and graphene hybrid nanostructures. Cu-graphene hybrid nanofluid was successfully synthesized by dispersing the synthesized Cu and graphene nanostructures (keeping the Cu concentration constant at 0.04 vol % and varying the graphene concentration from 0.01 to 0.1 vol %) in water. Hybrid nanofluids display excellent stability against aggregation for up to 7 weeks, as proven by higher zeta potential values. Thermophysical characteristics of the prepared hybrid nanofluids were effectively measured. The thermal conductivity of Cu-graphene hybrid nanofluids shows exceptional enrichment (~ 35%) at minimal concentrations of hybrid nanostructures. Viscosity of the water-based hybrid nanofluids shows remarkable enhancement as compared to water and represents the increasing trend in viscosity of the base fluid with respect to the increase in concentration of hybrid nanostructures. The thermal and rheological properties of hybrid nanofluids are effectively validated with existing theoretical models. In addition, the specific heat and pumping power of Cu-graphene hybrid nanofluids with respect to the volume concentration of hybrid nanostructures are calculated using the existing theoretical equations. A figure of merit (FOM) analysis was conducted for the synthesized hybrid nanofluids to gauge thermal efficiency and evaluate the applicability of these hybrid nanofluids under laminar and turbulent flow conditions.

List of symbols

k	Thermal conductivity (W m^{-1} K)
T	Temperature (°C, K)
$\varnothing$	Volume concentration (%)
n	Shape factor
μ	Viscosity (mPa.s)
C_p	Specific heat (J kg^{-1}.)
ρ	Density (kg m^{-3})
$\dot{m}$	Mass flow rate (kg s^{-1})
ΔP	Pressure drop (Pa)
D	Nanoparticle crystal size (nm)
β	Full width at half maximum (FWHM),
λ	X-ray wavelength (Å, nm)
θ	Bragg's angle (degrees)
d	Interplanar spacing (nm)

Abbreviations

RPM	Rotation per minute
FESEM	Field emission scanning electron microscope

✉ Müslüm Arıcı
muslumarici@gmail.com

✉ Mohammed Rehaan Chandan
chandan1816@gmail.com

[1] Colloids and Polymers Research Group, School of Chemical Engineering, Vellore Institute of Technology, Vellore, Tamil Nadu 632014, India

[2] School of Mechanical Engineering, Vellore Institute of Technology, Vellore, Tamil Nadu 632014, India

[3] Mechanical Engineering Department, Engineering Faculty, Kocaeli University, Umuttepe Campus, Kocaeli 41001, Turkey

M$_o$	Mouromtseff number
PVP	Polyvinylpyrrolidone
SDS	Sodium dodecyl sulfate
XRD	X-ray diffraction
UV-vis	Ultraviolet—visible
FOM	Figure of merit
ASTM	American society for testing and materials

Subscripts

hnf	Hybrid nanofluid
nf	Nanofluid
bf	Base fluid
np	Nanoparticle

Introduction

Hybrid nanofluids have emerged as a fascinating group of advanced fluids with tremendous potential for various applications due to their unique properties and enhanced performance. These innovative fluids are obtained by dispersing more than one nanostructure and other additives in a base fluid, exhibiting exceptional thermal, electrical, and optical properties, making them highly attractive for a wide range of industries and research fields [1, 2]. Hybrid nanofluids find applications in diverse areas, including heat transfer enhancement [3, 4], energy conversion [5], electronics cooling [6], biomedical engineering [7], battery cooling [8], and solar energy systems [9]. In heat transfer applications, hybrid nanofluids have demonstrated superior thermal conductivity and convective heat transfer coefficients, leading to enhanced efficiency and performance of heat exchangers, refrigeration systems, and cooling devices. Additionally, these nanofluids have shown promise in improving the efficiency of solar collectors, thermoelectric devices, and hemodynamics applications [9–12], thus contributing to sustainable energy generation. Abdelrazek et al. [13] synthesized alumina-coated MWCNT hybrid nanofluid using two step method to check its thermal performance in an annular passages under fully developed turbulent flow conditions. Hussein et al. [14] prepared water-based titanium dioxide and functionalized multi-walled carbon nanotube-based hybrid nanofluid for using in flat plate solar applications. Moreover, their unique electrical and optical properties enable their utilization in electronic devices, sensors, and photonic applications, further expanding their potential impact [15]. Furthermore, the visualization of electroosmotic flow of immiscible fluids through a porous medium in vertical annular microtubes was also performed using numerical simulations in order to suggest the kerosene based hybrid nanofluids in oil flow applications [16].

The synthesis of hybrid nanofluids involves the careful selection of nanoparticles and additives, followed by their dispersion in a base fluid. Various synthesis techniques, such as two-step, one-step, and surface functionalization, have been developed to ensure the uniform distribution and stability of nanoparticles in the fluid. From the literature, it has been identified that methods such as synthesis by wet chemical method [17], vapor deposition by chemical process (CVD) [18], wet mechanical grinding technique [19], mechanical ball milling, reduction of metal ions by chemical reduction process, and hot-wire system [20, 21] usually regarded as one step methods for the synthesis of hybrid nanofluids. However, understanding the underlying mechanisms governing stability is essential to ensuring long-term stability, preventing particle settling, and avoiding clogging or fouling issues in the fluidic systems. In addition, manufacturing hybrid nanofluids with remarkable enhancements in thermophysical properties is challenging. To assess the performance of hybrid nanofluids, several thermophysical characterizations are conducted. These include measurements of thermal conductivity, viscosity, density, and specific heat capacity. These properties are considered to be essential in understanding the behavior of nanofluids and evaluating their potential for specific applications. Table 1 shows the literature review that includes an explanation of the main themes that were used by researchers to generate mono and hybrid nanofluids using either a one-step procedure or a two-step technique. The study findings on hybrid and nanofluids in heat transfer investigations are covered in the literature below.

Furthermore, from Table 1, we can observe that very limited works have been conducted on figure of merit analysis (FOM) which serves as to calculate overall execution and is often employed to compare and rank different nanofluid formulations. Figure of merit (FOM) is an index used to describe the performance of a process. Heat transfer fluid efficacy is evaluated using FOM. FOM is used to correlate the heat transfer coefficients of the base fluid and the nanofluid, for evaluating the thermal efficiency of a nanofluid. The suggested nanofluid suitability in laminar or turbulent flow regions can be decided based on FOM. If the FOM value is greater than one, then the nanofluid can be considered as better heat transfer fluid in any flow region. This analysis considers a combination of properties and provides a quantitative assessment of the nanofluid's suitability for a particular application [11, 25, 27]. Samarshi et al. [31] conducted FOM analysis for TiO$_2$ nanofluids and showed better heat transfer capability of these nanofluids under internal laminar flow. Elcioglu et al. [33] stated that the FOM was characterized using the Mouromtseff number (M$_o$) and also reported that hybrid nanofluids show better thermal performance as compared to base fluids provided the Mo number greater than one.

Considering the discussion previously mentioned, it has been noted that most of the work was conducted on

Table 1 A review of the literature on hybrid and mono nanofluids

References	Hybrid nanoparticle	Volume concentration	Base fluid	Synthesis method	Dispersant and stability	Thermophysical property (% enhancement)		Heat transfer studies	FOM
						Thermal conductivity	Viscosity		
Tong et al. [5]	MWCNT–Fe_3O_4	0.005–0.2 mass%	EG/deionized water (20:80)	Two-step method	Citric acid	3.8%	Not done	Yes	No
Wang et al. [6]	Al_2O_3–Cu–TiO_2	0.1—0.5 vol%	DI-water	Two-step method	PVP	12.5%	Not done	Yes	No
Struchalin et al. [9]	Fe_3O_4-MWCNT	0.098 vol%	Water/Ethanol	Two-step method	SDS	Not done	Not done	Yes	No
Suresh et al. [22]	Al_2O_3_Cu	0.1% to 2%	Water	Two-step method	SLS	12.11%	78%	No	No
Abbasi et al. [23]	γAl_2O_3–MWCNT	0.2–1 vol%	Water	Two-step method	GA	14.7%	Not done	No	No
Tiwari et al. [24]	CeO_2+MWCNT	0.25–1.5 vol%	Silicone Oil	Two-step method	BAC	Not done	64%	No	No
Mane et al. [25]	CuO+Fe_3O_4	0.1 mass%	Water	Two-step method	Chitosan	4.9%	10%	Yes	Yes
Kanti et al. [26]	GO–TiO_2	0.05–1.0 vol%	Distilled water	Two-step method	PVP	7.97%	37%	Yes	No
Kanti et al. [27]	Fly ash–Cu	0.5—4.0 vol%	Distilled water	Two-step method	Triton X-100	13.1%	45.18%	Yes	Yes
Phanindraa et al. [28]	Al_2O_3–Cu	0.1vol. %	Transformer oil	Two-step method	No	27%	35%	Yes	No
Kumar and Sarkar [29]	Al_2O_3–MWCNT	0.01 vol%	Water	Two-step method	No	0.6%	8.8%	Yes	No
Mostafizura et al. [30]	Al_2O_3_MWCNT	0.1–0.5 vol%	Radiator coolant	Two-step method	SDS	13.7%	11%	Yes	Yes
Samarshi et al. [31]	TiO_2	10–100 ppm	Water	Two-step method	PVP, Tween 20	8.3%	50%	Yes	Yes
Das et al. [32]	Graphene	0.02–0.1 mass%	Water	Two-step method	Gum Acacia	17%	175%	Yes	No

oxide-based hybrid nanofluids using high concentrations of nanostructures to enhance the thermophysical properties. Although hybrid nanofluids are synthesized using oxide-based nanostructures to enhance the thermal conductivity of base fluid in literature, the percentage enhancement in thermal conductivity is not up to the mark due to the low thermal conductivity of oxide structures. Hence, it is very essential to develop a suitable hybrid nanofluid using non-oxide based nanostructures for enhancing the thermophysical properties of base fluids. In this work, we propose metal and graphene-based hybrid nanofluid, such as Cu-graphene hybrid nanofluid, by dispersing a very low concentration of Cu and graphene nanostructures in water for enhancing thermophysical characteristics of the base fluid. Cu and graphene are selected as suitable non oxide based materials such as metal and carbon-based material due to its high thermal conductivity. Moreover, thermal performance estimation of hybrid nanofluids using FOM analysis is also focused on suggesting the developed hybrid nanofluid under various internal flow conditions, which is very sparse in the literature.

Experimental

Materials required

Copper (II) chloride dihydrate ($CuCl_2.2H_2O$), graphite powder (<20 μm), hydrogen peroxide (30% H_2O_2), sodium chloride (NaCl), and hydrazine hydrate reagent grade (N_2H_4) were obtained from Sigma-Aldrich, India. Polyvinylpyrrolidone (PVP K-30) was procured from SRL, India. Ammonia solution 25% AR grade and sulfuric acid (98% H_2SO_4) were purchased from SD Fine Chemicals, India. Absolute ethanol was supplied by Changshu Hongsheng fine chemicals, China
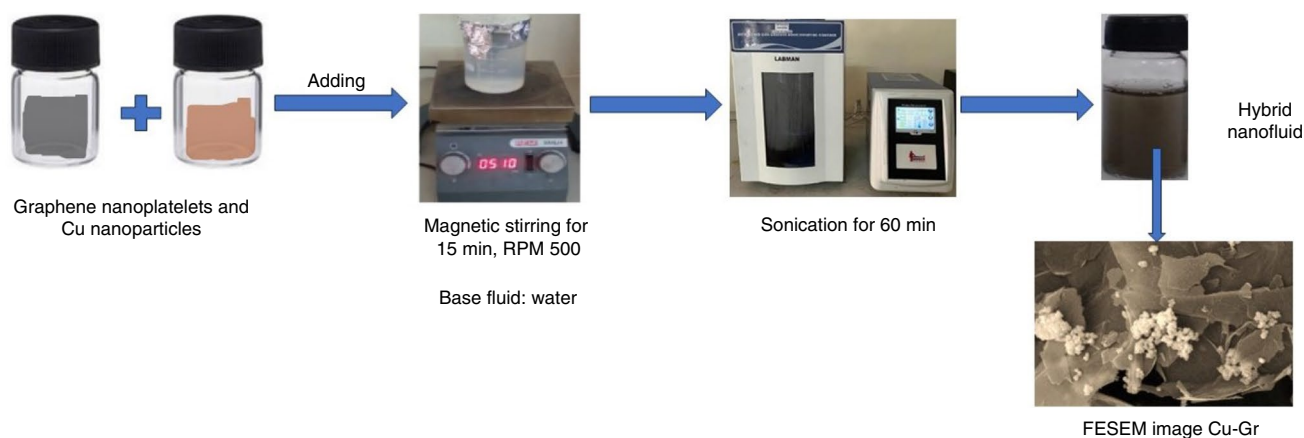
Fig. 1 Two-step synthesis of water-based Cu-graphene hybrid nanofluid

(Xilong Scientific). Substances obtained have been utilized directly after purchase without any treating procedures.

Water has been employed as a base fluid for synthesizing Cu nanoparticles and hybrid nanofluids. Due to the easily oxidizable nature of Cu, it is crucial to make the base fluid free of oxygen. Hence, water was degassed with inert gas for 20 min to remove the dissolved oxygen present in the base fluid.

Synthesis of Cu nanopowder

Cu nanopowder was produced altering the procedure developed by Chowdhury et al. [34]. This method initially involves the preparation of Cu nanoparticles in the water phase using the chemical reduction method, followed by centrifugation of Cu sol at 10,000 rpm to produce Cu nanopowder. Briefly, the polyvinylpyrrolidone aqueous solution was produced by adding 2 g PVP powder to 100 mL of degassed water, followed by stirring. Later, it was stirred continuously by mixing 0.25 g of copper chloride dihydrate into the mixture for 10 min. Then, the pH of the solution was tuned to 11 by slowly adding ammonia solution. After the pH adjustment, the color immediately changed to blue. Then, it was stirred continuously for 1 h at 50 °C in water bath. After 1 h, the reduction of the solution was conducted by adding 20 mL of 0.6 M hydrazine hydrate solution. Following the reduction process, the color turned to copper brown which designates the generation of Cu nanoparticles in the water phase. Finally, Cu nanopowder was separated from aqueous Cu sol by centrifuging the aqueous sol at 10,000 rpm for 20 min. After 20 min, Cu nanoparticles stuck at the bottom of the centrifuge vial. The stuck Cu nanoparticle powder was separated from the supernatant and dried using a vacuum oven at 50 °C for 5 h. After drying, Cu nanoparticle powder was recovered from the centrifuge vial by grinding the dried flakes using a glass rod.

Synthesis of graphene nanoplatelet powder

Tran et al. [35] synthesized graphene by thermal treatment and grinding technique. The same protocol is used in this work for producing graphene. In the first step, thermal treatment of graphite powder was performed by pretreating the graphite powder with the mixture of H_2O_2 (30%) and H_2SO_4 (98%) in 1:1.5 (v/v) ratio for 2 h at a temperature of 20 °C. Later, the solid mass present in the above solution was filtered and washed with distilled water until the pH reduces to 7. After washing, the final solid mass is dried at 80 °C for 10 h to produce the expanded graphite. Finally, the above-produced expanded graphite was ground with NaCl in a 3:1 molar ratio using a planetary ball mill at 350 rpm under an inert gas environment for 2 h. The NaCl present in the mixture was removed by washing with distilled water. The final sample containing the graphene nanoplatelets was collected by drying at 70 °C under a vacuum oven for 4 h.

Synthesis of Cu-graphene hybrid nanofluid

Cu-graphene hybrid nanofluids were manufactured by dispersing the already synthesized Cu nanoparticles and graphene nanoplatelets powders in the base fluid using the ultra-sonication method. Briefly, Cu-graphene hybrid nanofluid was synthesized by adding 0.02 vol % of Cu nanoparticle powder along with graphene nanoplatelets powder in water followed by magnetic stirring for 15 min with 500 RPM and the probe sonication for 60 min. After sonication, stable water-based Cu-graphene hybrid nanofluid was obtained successfully. Here, Cu nanoparticle powder concentration was kept constant at 0.04 vol % in all the samples of hybrid nanofluids by varying graphene nanoplatelets powder concentration (0.01, 0.025, 0.05, 0.075, and 0.1%) (Fig. 1).

Nanoparticle and nanofluid characterization

Cu-graphene hybrid nanofluids were tested for their thermophysical properties using various techniques. Hybrid nanofluid density was measured using the specific gravity (or) density bottle method. Thermal property of hybrid nanofluids such as thermal conductivity was determined utilizing KD2 Pro thermal conductivity meter (Decagon Devices Inc) which uses hot-wire method. The suspension viscosity was measured using the DV2TLV AMETEK Brookfield viscometer, USA. The optical property of Cu nanoparticles and graphene nanoplatelets is measured by a UV–vis spectrophotometer (SHIMADZU 1800). The colloidal stability of Cu-graphene hybrid nanofluids was tested employing sedimentation photography and zeta potential analysis (HORIBA SZ-100, version 2.00). The morphology of Cu nanoparticles and graphene nanoplatelets was identified using field emission scanning electron microscope (FESEM, ZEISS). The phase purity of copper, graphene, and Cu-graphene nanostructures was characterized by the X-ray diffraction (XRD) technique using Cu Kα radiation (Bruker D8 Advance, Germany).

Results and discussion

Using XRD, FESEM, and UV–vis spectroscopy, respectively, the structural, morphological, and optical responses of nanomaterial and hybrid composite were fully investigated. In order to evaluate a sample's electrical structure, UV–vis spectroscopy measures how much light is absorbed in the ultraviolet area. FESEM is used to acquire high-resolution topographic images of surface sample, while XRD is utilized to identify the crystal structure of a sample by analyzing the diffraction pattern of X-rays that are scattered by the atoms in the sample.

Material characterization

Cu Kα X-rays were used to perform an XRD analysis on the produced sample of nanoparticles, and data were gathered for the 2θ range of 10°–80°. The synthesized samples were originally examined using X-ray diffraction (XRD) to determine a material's crystalline structure. Figures 2a, b, and c show the XRD patterns of copper, graphene, and hybrid Cu-graphene, respectively. Figure 2a shows that the copper nanomaterial's XRD pattern exhibits diffraction peaks at 42.5°, 49.8°, and 73.5° that are associated with the 111, 200, and 220 phases of pure copper with a face-centered cubic (FCC) crystal structure. Cu is an effortlessly oxidizable metal, hence surface oxidation is a possibility. The development of a Cu_2O layer on nanoparticle surface together with pure Cu peaks is seen by a minor peak in XRD investigations

at diffraction angles of 35.5°, 36°, and 38° (highlighted in Fig. 1a) [20] with JCPDS card no. 00–004-0836. The graphene nanoplatelet powder diffraction peaks are displayed in Fig. 2b with the standard JCPDS Card No. 01-075-2078 at 26.3 with a (003) lattice and at 54.3 with (006). As can be observed in Fig. 2c, the phase purity of hybrid nanostructures containing hybrid Cu–Gr was also evaluated using the XRD analysis.

The following equation presents the Scherrer equation, which is used to determine the nanoparticles' crystal size (D):

$$D = \frac{0.9\lambda}{\beta \cos\theta} \tag{1}$$

where β is the full width at half maximum (FWHM), λ is 1.54056 Å for X-rays wavelength, and θ is the Bragg's angle for a specific diffraction plane are used.

The interplanar spacing (d) is calculated by using Bragg's law:

$$n\lambda = 2d\sin\theta \tag{2}$$

where n is the order of reflection, λ is X-rays wavelength used for the diffraction experiment, d is the interplanar spacing, and θ is the Bragg angle.

Calculated average crystal size (D) and interplanar spacing (d) for copper nanoparticles and graphene nanoplatelets are tabulated in Table 2.

Particle morphology

Field emission scanning electron microscopy (FESEM) investigation is utilized to evaluate the morphology and form of the nano and hybrid composite. The copper nanoparticles visible in the FESEM picture shown in Fig. 3b are in spherical shape, with an average diameter of around 60 nm. Graphene represents flake-like structures as depicted in Fig. 3c, and the structure of the Cu-Gr hybrid nanostructures is shown in Fig. 3f, displaying the deposition of Cu nanoparticles on grapheme nanoplatelets.

Optical properties of Cu, graphene, and Cu-graphene hybrid nanofluids

Optical properties Cu, graphene, and Cu-graphene hybrid nanofluids are measured by means of UV–vis spectrophotometer as shown in Fig. 4. UV–vis of the Cu sample (from Fig. 4a) shows a peak at 582 nm which corresponds to the pure Cu nanoparticles with no traces of oxide peaks of Cu nanoparticles. Another characteristic peak at 263 nm [36] from Fig. 4b represents the graphene peak indicating the dispersion of graphene nanostructures
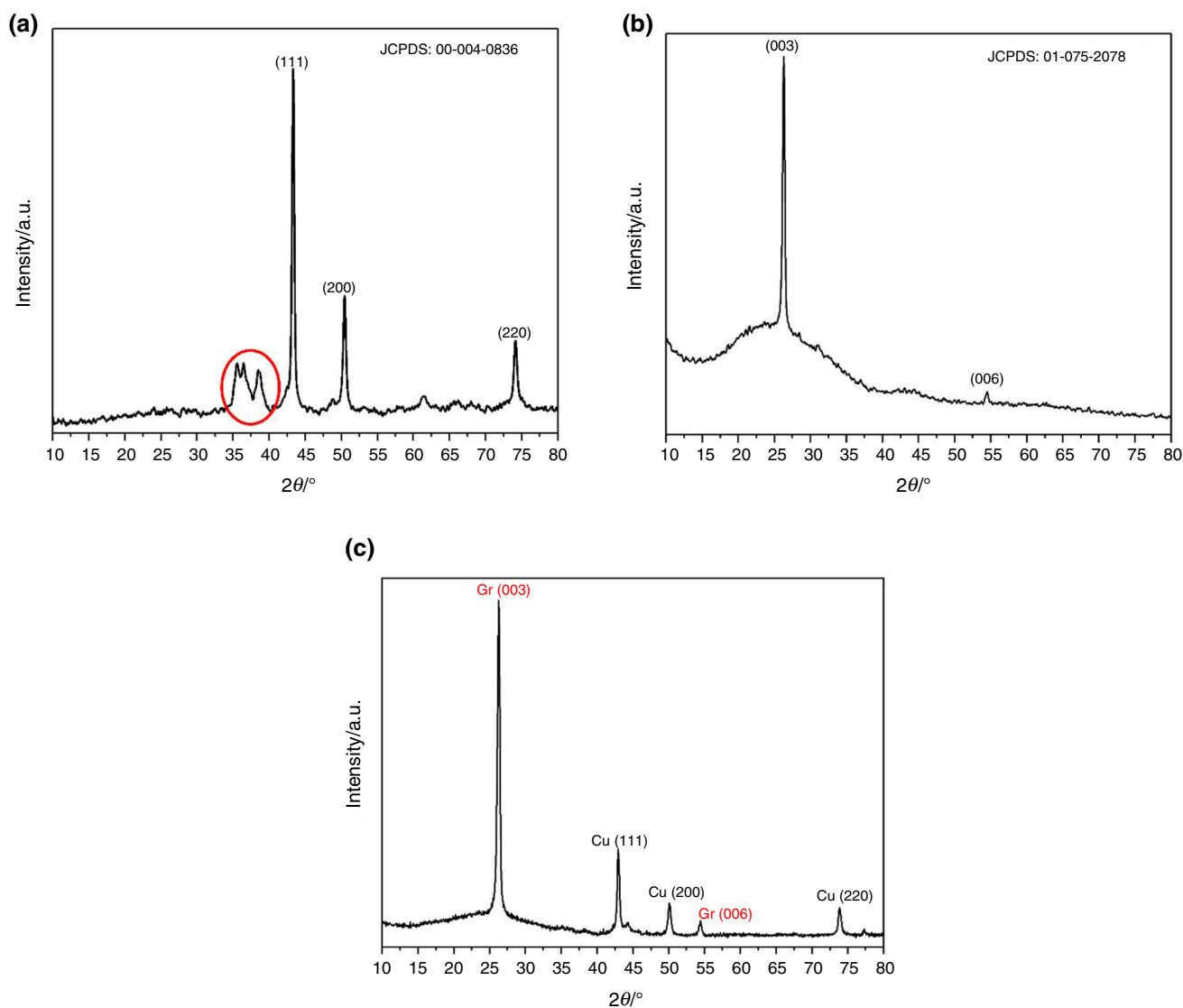
Fig. 2 XRD of (**a**) copper nanoparticles, (**b**) graphene nanoplatelets, and (**c**) hybrid Cu-Gr

Table 2 The crystal size of Cu and graphene nanostructures calculated from XRD data

Sample	Average crystal size (D) nm	Average inter-planar spacing (d) nm
Copper nanoparticles	20.52	0.212
Graphene nanoplatelets	17.62	0.241

in water. Cu-graphene hybrid nanofluids displays the both surface plasmon resonance peaks of copper and graphene (Fig. 4c), suggesting the proper formation of Cu-graphene hybrid nanofluids in water.

Stability analysis of Cu-graphene hybrid nanofluids

Cu-graphene hybrid nanofluids stability was tested using both sedimentation photography and zeta potential measurements. Stability of nanofluids plays a critical role in determining the long-term operational feasibility of nanofluids and provides clarity of particle aggregation and sedimentation-related issues which can affect both thermal properties and heat transfer performance. Therefore, it is very important to study the stability of hybrid nanofluids over time.

In the first technique, the possible settling of nanostructures in base fluid at different time intervals has been observed and documented using digital photographs as displayed in Fig. 5. It has been observed that the hybrid nanofluid suspension is highly stable for at least 7 weeks without
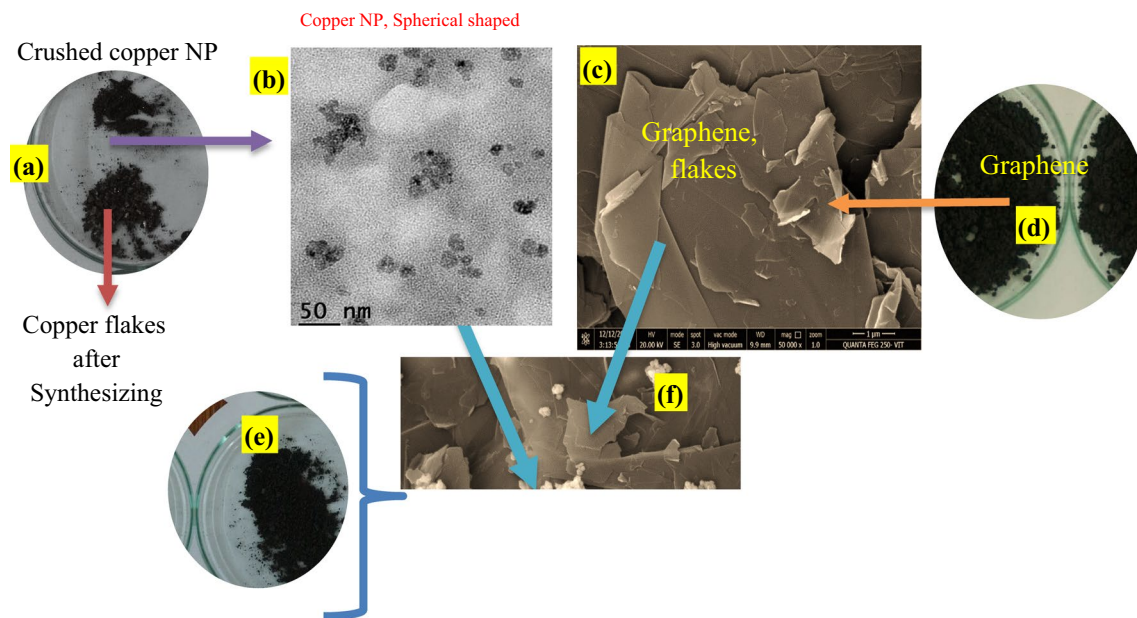
Fig. 3 **a** Digital photo image of powdered Cu nanoparticles, **b** TEM image of Cu nanoparticles, **c** FESEM image of graphene nanoplatelet, **d** Digital photo image of graphene nanoplatelet, **e** Digital photo image of hybrid Cu-Gr nanomaterial, and **f** FESEM image of hybrid Cu-Gr nanomaterial

aggregation or sedimentation of nanoparticles at the bottom of the vial.

In addition to the visual observation of the nanofluid stability at different time intervals, the zeta potential analysis was conducted to further assess the stability over time. Zeta potential analysis is an important technique where the stability of nanofluids is measured by quantifying the charge present on the electrical double-layer surface of nanostructures. A higher value of zeta potential ($> \pm 30$ mV) represents the better stability of nanofluids. Table 3 shows the zeta potential of Cu-graphene hybrid nanofluids prepared by varying the graphene nanoplatelet concentration and keeping constant Cu concentration. From the table, it has been observed that all the samples show higher negative zeta potential values. However, decrease in the zeta potential values was also detected due to the increase in the concentration of graphene nanoplatelets after 7 weeks. Such trends in the zeta potential value could be possibly due to the particle aggregation over time and increased concentration of nanostructures.

Thermophysical properties of Cu-graphene hybrid nanofluids

The thermophysical properties of Cu-graphene hybrid nanofluids were tested through various techniques or calculated theoretically. The thermal conductivity, density, and viscosity of hybrid nanofluids were characterized using different testing instruments as mentioned in Sect. 2.5, whereas the specific heat was calculated theoretically by existing equations available in the literature. Detailed analysis of these properties has been discussed in the subsequent section.

Density of Cu-graphene nanofluids

The density of nanofluids is considered as major thermophysical property as it influences the pumping power and pressure drop associated with the transportation of fluids in heat-exchanger devices. Hence, it is very important to study the variation of density at different particle concentrations. Figure 6 shows the consequence of nanoparticle concentrations on the density of the hybrid nanofluid. From the figure, it can be seen that the density of the water-based Cu-graphene hybrid nanofluids increases with an increase in the concentration of Cu nanoparticles and graphene nanoplatelets, which is consistent with the work reported by other researchers [4, 37–39].

Thermal conductivity of hybrid nanofluids

Thermal conductivity is considered to be an important thermophysical property that indicates the thermal performance potential of any nanofluid. It is always desirable to have higher thermal conductivity for a coolant to exhibit better thermal performance. Figure 6 depicts the effect of the nanoparticle concentration (Cu-graphene) on the thermal conductivity of hybrid nanofluid and its enhancement as compared to conventional base fluid such as water.
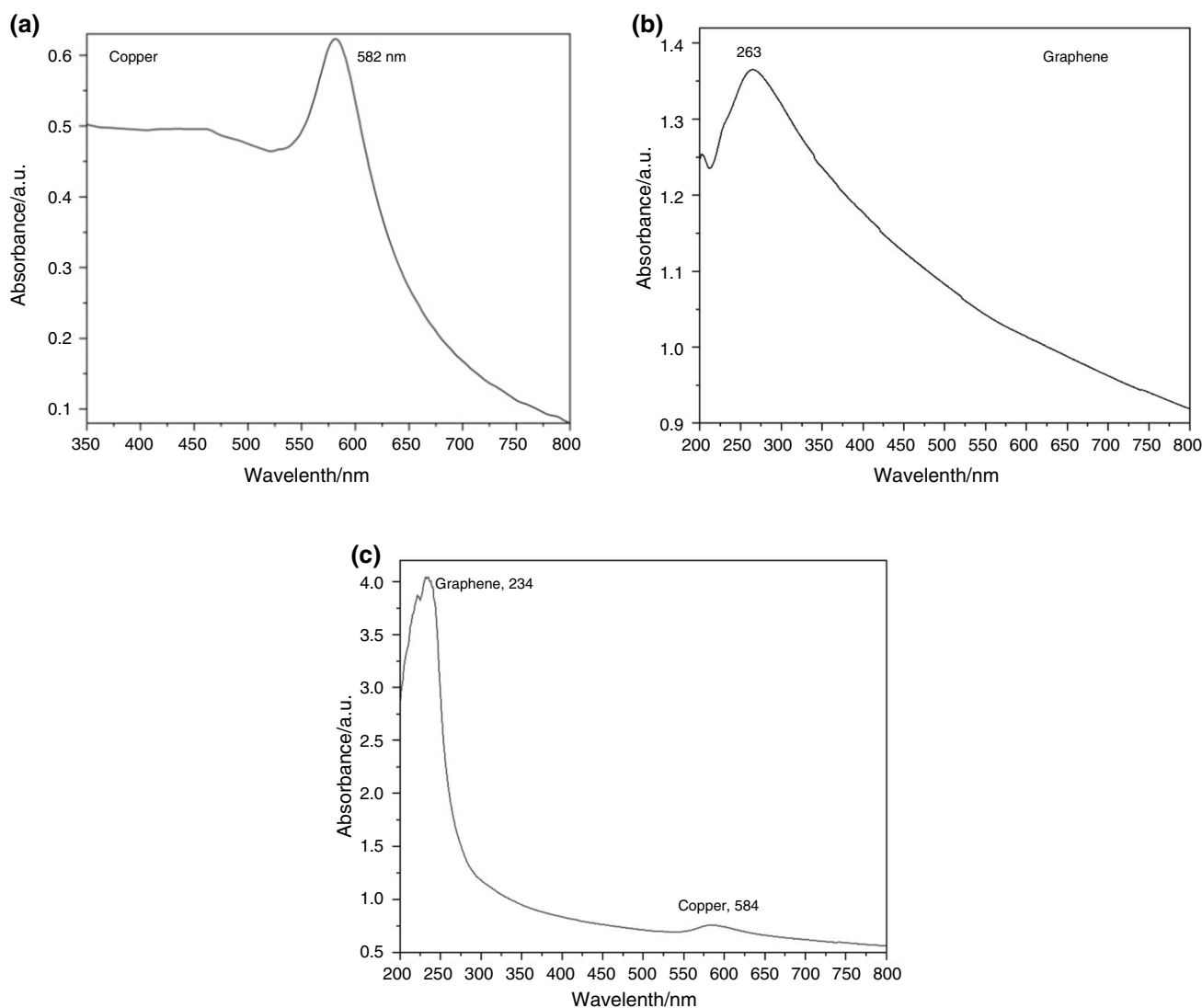
Fig. 4 UV–Vis plot of (**a**) copper nanoparticles, **b** graphene nanoplatelets, and **c** Cu-graphene hybrid nanostructures dispersed in water

From Fig. 7a, it can be observed that the thermal conductivity of water-based hybrid nanofluid increases with an increase in the hybrid nanoparticle loading. The possible reason for rise in thermal conductivity could be due to the metallic nature of copper, the 2D structure of graphene, and the high stability of hybrid nanofluid at different particle concentrations as seen from the zeta potential measurements. Further, the percentage enhancement in thermal conductivity of hybrid nanofluid at different particle loading was calculated and shown in Fig. 7b. The percentage enhancement in thermal conductivity of hybrid nanofluid was found to increase with an increase in the concentration of hybrid nanostructures. It represents higher enhancement ($\sim 35\%$) in the thermal conductivity at high particle loading (~ 0.14 vol %). Moreover, the experimentally measured thermal conductivity is also validated using the existing theoretical models such as the modified Maxwell, Hamilton Crosser, and Yu and Choi model as shown in Fig. 7c. According to these models, the thermal conductivity of nanofluid is dependent on several factors like thermal conductivity of nanoparticles & base fluid, particle concentration, clustering effect, and shape factor as shown below. Details of these models are given in Table 4.

Here, $\varnothing$ is the total volume concentration of hybrid nanostructures, $\varnothing_{np1}$ and $\varnothing_{np2}$ are the volume concentrations of nanoparticle 1 (copper) and nanoparticle 2 (graphene nanoplatelet). On the other hand, k_{hnf}, k_{bf}, k_{np1} and k_{np2} are the thermal conductivity of hybrid nanofluid, base fluid, nanoparticle 1, and nanoparticle 2, respectively. Whereas n_1 and n_2 are the shape factor constituents of the first and second particles, respectively. Finally, β represents the clustering effect.

Fig. 5 Stability analysis of water-based Cu-graphene nanofluids at different time intervals: **a** after preparation, **b** after 1 week, **c** after 2 weeks, **d** after 3 weeks, **e** after 4 weeks, **f** after 5 weeks, and **g** after 7 weeks
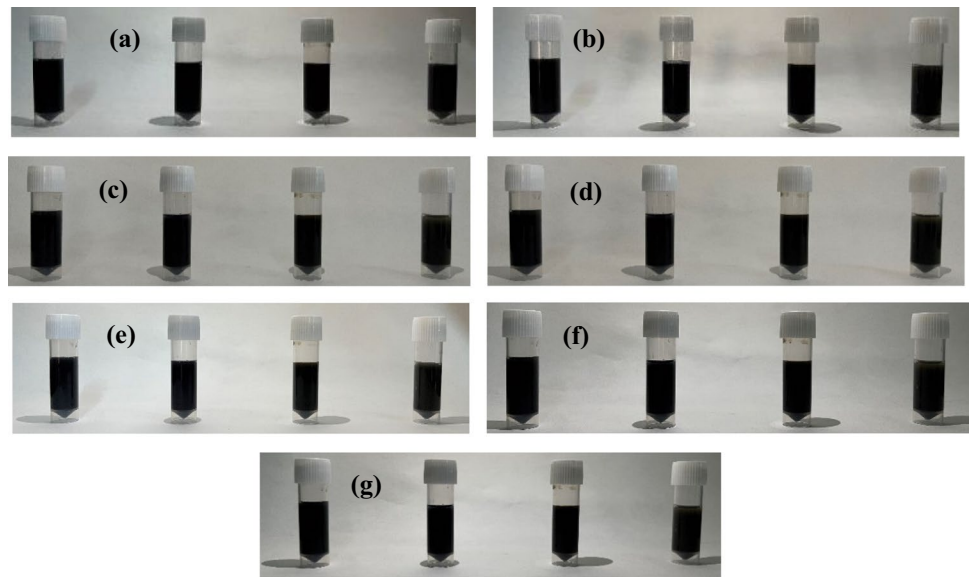

Table 3 Zeta potential values of Cu-graphene hybrid nanofluids as a function of time and concentration

S. No.	Cu: Graphene concentrations (vol %)	Zeta potential on day 0 (mV)	Zeta potential on day 49 (mV)
1	0.04:0.025	−69.9	−65.5
2	0.04:0.05	−57.8	−53.1
3	0.04:0.075	−56.2	−51.2
4	0.04:0.1	−53.1	−48.4
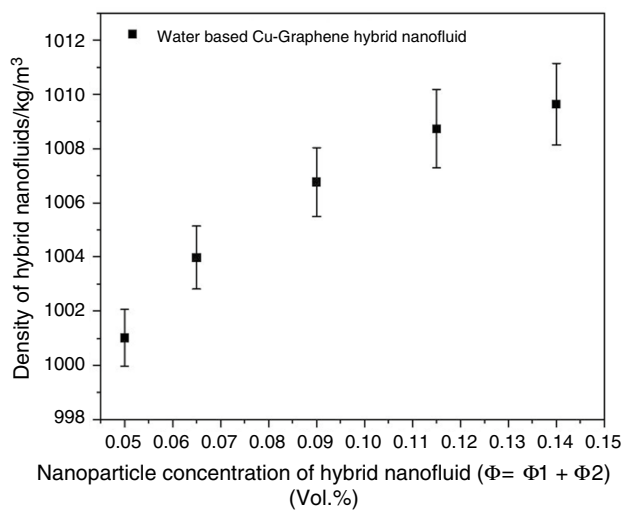
Fig. 6 Effect of Cu-graphene hybrid nanostructures concentration on the density of hybrid nanofluid

From Fig. 7c, it can be seen that the thermal conductivity of water-based hybrid nanofluid moderately fits with R^2 of 0.86088 with the Yu and Choi model which considers the clustering effect. On the other hand, the modified Maxwell and Hamilton model fails to fit the experimental thermal conductivity data. This could be due to ignoring key parameters such as particle size, clustering effect, and the particle-liquid interface interactions in the conventional models which plays a major character in improving the thermal conductivity.

Viscosity of hybrid nanofluids

Viscosity is another vital parameter that plays a crucial role in transporting the nanofluids and deciding the pumping power requirements. Hence, it is very much essential to study the effect of the concentration of hybrid nanostructures on the viscosity and base fluid. Figure 8 represents the rheological behavior of hybrid nanofluids for different concentrations of hybrid nanostructures in the base fluid. From Fig. 8a, it has been observed that the viscosity of hybrid nanofluid increases with an increase in the concentration of Cu-graphene nanoparticles. A remarkable enhancement in viscosity (~65%) has been reported as compared to water (base fluid) which could be possibly due to the interaction of base fluid molecules with hybrid nanostructures [24, 44, 45]. Moreover, experimental viscosity data of hybrid nanofluids have also been validated with existing theoretical models such as Pak and Cho [46], Brinkman [47], Einstein [48], Akilu et al. [49], Chen et al. [50], and Batchelor [51] models as shown in Fig. 8b.

Pak and Cho model [46]*:*

$$\mu_{\text{hnf}} = \mu_{\text{bf}}\left(1 + 39.11 \times \varnothing + 533.9 \times \varnothing^2\right) \tag{3}$$
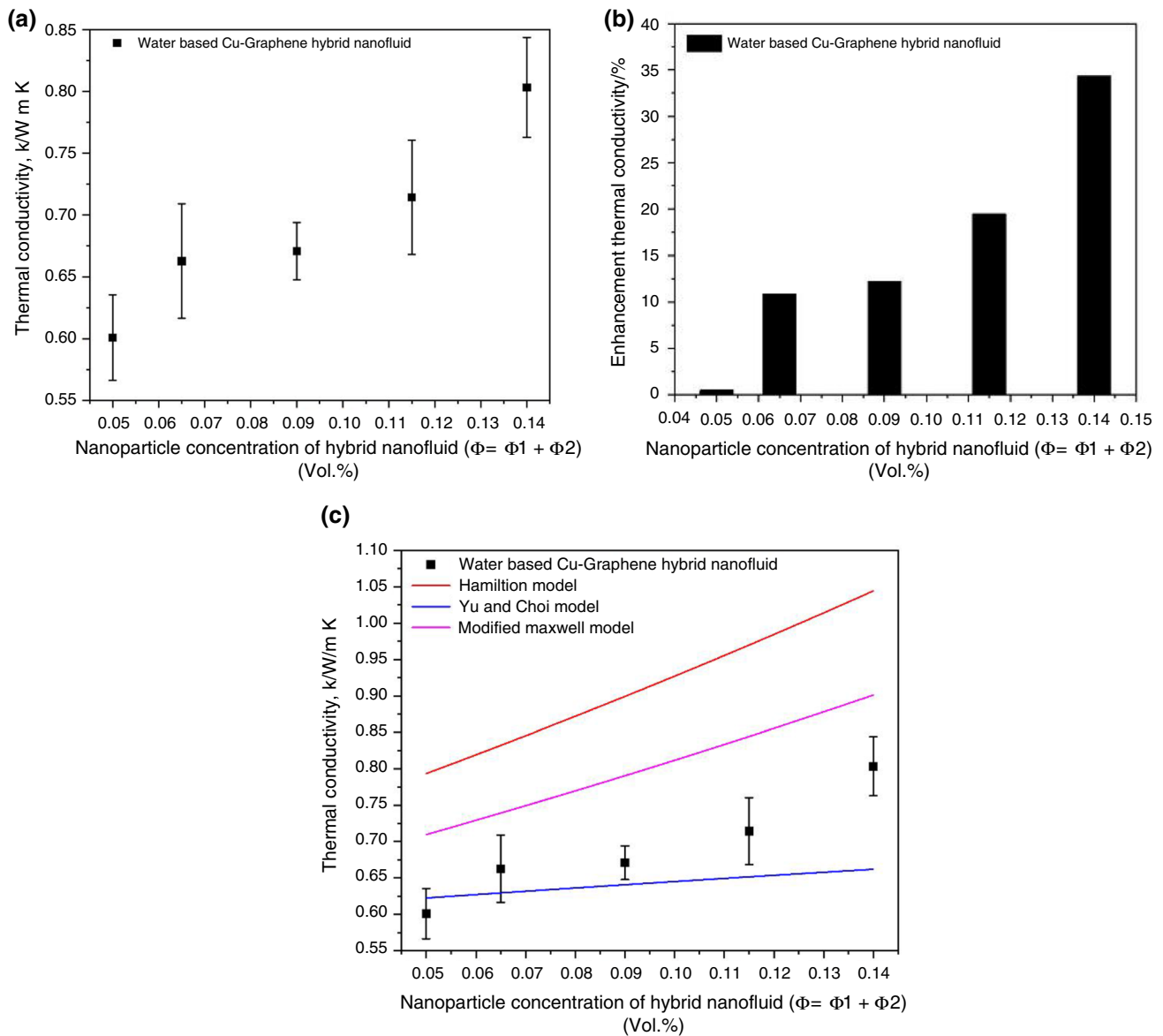
Brinkman model [47]*:*

Fig. 7 Effect of concentration of Cu-graphene hybrid nanostructures on (**a**) thermal conductivity (**b**) the enhancement of thermal conductivity in hybrid nanofluids, and **c** validation of experimental thermal conductivity data with the existing model equations

Table 4 different theoretical models collected from the literature

Model	Equation	References	Equation no.
Modified Maxwell model	$k_{hnf} = k_{bf} \left[\dfrac{\frac{(\varnothing_{np1} k_{np1} + \varnothing_{np2} k_{np2})}{\varnothing} + 2k_{bf} + 2((\varnothing_{np1} k_{np1} + \varnothing_{np2} k_{np2})) - 2\varnothing k_{bf}}{(\frac{(\varnothing_{np1} k_{np1} + \varnothing_{np2} k_{np2})}{\varnothing}) + 2k_{bf} - (\varnothing_{np1} k_{np1} + \varnothing_{np2} k_{np2}) + \varnothing k_{bf}} \right]$ $\varnothing = \varnothing_{np1} + \varnothing_{np2}$	[40, 41]	(1)
Hamilton and Crosser model	$k_{hnf} = k_{bf} \left[\dfrac{k_{np1} + (n_1 - 1)k_{bf} - (n_1 - 1)\varnothing_{np1}(k_{bf} - k_{np1})}{k_{np1} + (n_1 - 1)k_{bf} + \varnothing_{np1}(k_{bf} - k_{np1})} \right] *$ $\left[\dfrac{k_{np2} + (n_2 - 1)k_{bf} - (n_2 - 1)\varnothing_{np2}(k_{bf} - k_{np2})}{k_{np2} + (n_2 - 1)k_{bf} + \varnothing_{np2}(k_{bf} - k_{np2})} \right]$	[40, 42]	(2)
Yu and Choi model	$\dfrac{k_{hnf}}{k_{bf}} = \left(\dfrac{(k_{np2} + 2k_{bf} - 2\varnothing(k_{bf} - k_{np})(1+\beta)^3)}{(k_{np2} + 2k_{bf} - \varnothing(k_{bf} - k_{np})(1+\beta)^3)} \right)$	[40, 43]	(3)

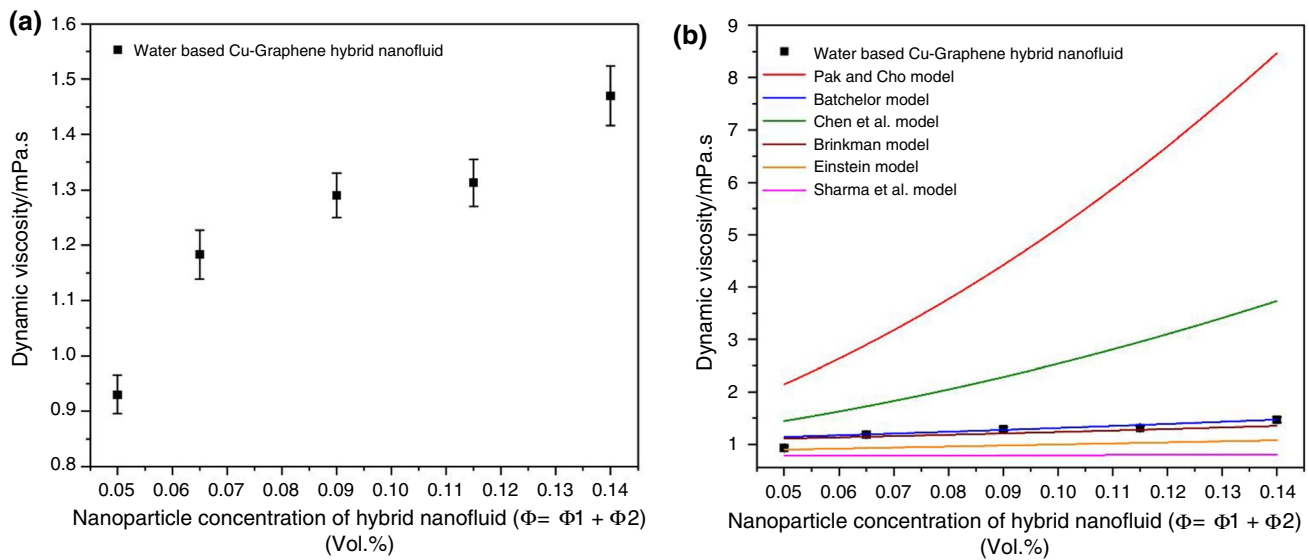**Fig. 8** **a** Effect of Cu-graphene hybrid nanostructures concentration on the viscosity of hybrid nanofluid and **b** Validation of experimental viscosity data with the existing model equations

$$\mu_{hnf} = \mu_{bf}\left(\frac{1}{(1-\varnothing)^2}\right) \tag{4}$$

Einstein model [48]:

$$\mu_{hnf} = \mu_{bf}(1 + 2.5 * \varnothing) \tag{5}$$

Akilu *et al.* model [49]:

$$\mu_{hnf} = \mu_{bf}\left(0.9653 + 77.4567\left(\frac{\varnothing_{hnf}}{100}\right)^{1.1558}\left(\frac{T_1}{T_2}\right)^{0.6801}\right) \tag{6}$$

Chen et al. model [50]:

$$\mu_{nf} = \mu_{bf}(1 + 10.6 * \varnothing + (10.6 * \varnothing)^2) \tag{7}$$

Batchelor model [51]:

$$\mu_{nf} = \mu_{bf}(1 + 2.5 * \varnothing + 6.2 * \varnothing^2) \tag{8}$$

Here, μ_{hnf} and μ_{bf} show the viscosities of hybrid and base fluids, and $\varnothing$ represents the total volume concentration of hybrid nanostructures. Whereas, T_1 and T_2 represent the initial and final temperature of the hybrid nanofluid, respectively.

From Fig. 8b, it can be seen that the Brinkman model with R^2 value of 0.97868 and Batchelor model with R^2 value 0.97872 fitted well with the water-based hybrid nanofluid.

Specific heat of hybrid nanofluids

In addition to density, viscosity, and thermal conductivity, specific heat is another important thermophysical property when considering the thermal performance of heat-exchanging devices. In this paper, the specific heat of Cu-graphene hybrid nanofluids is calculated using the already available theoretical equations from the literature as [11, 27] shown below:

$$(\rho C_p)_{hnf} = \varnothing_1(\rho C_p)_{s1} + \varnothing_2(\rho C_p)_{s2} + (1-\varnothing)(\rho C_p)_f \tag{9}$$

where, C_{phnf}, C_{ps1}, C_{ps2}, and C_{pf} indicate the specific heat of hybrid nanofluid, nanoparticle 1, nanoparticle 2, and base fluid. On the other hand, ρ_{hnf}, ρ_{s1}, ρ_{s2} and ρ_f signify the density of hybrid nanofluid, nanoparticle 1, nanoparticle 2, and base fluid, respectively. On the other hand, $\varnothing, \varnothing_1$, and $\varnothing_2$ denote the total volume concentration and volume concentration of nanoparticle 1 and nanoparticle 2 present in the base fluid, respectively.

Figure 9 shows the variation of calculated specific heat values of hybrid nanofluids at different concentrations of hybrid nanostructures. From the figure, it has been observed that the specific heat of Cu-graphene hybrid nanofluids decreases with an increase in the concentration of hybrid nanostructures. A similar trend was also reported by other researchers in the literature [11]. This could be possibly due to the low specific heat of Cu and graphene as compared to the base fluid. Moreover, the lower amount of energy available due to the increase in the concentration of hybrid nanostructures for activating the nanostructures is also responsible for the decrease in the specific heat.

Pumping power

Pumping power is another major parameter that is used in transporting hybrid nanofluids in heat-exchanging devices.
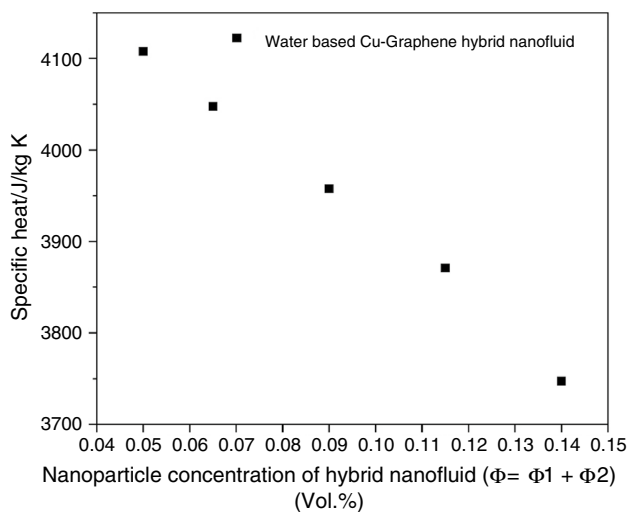
Fig. 9 Effect of Cu-graphene hybrid nanostructures concentration on the specific heat of hybrid nanofluid

Fig. 10 Effect of Cu-graphene hybrid nanostructures concentration on the pumping power of hybrid nanofluid

It is always desirable to have less pumping power for transporting the fluids. However, this strongly depends on the viscosity of hybrid nanofluids. The larger the viscosity of hybrid nanofluids, the greater the power required to pump the hybrid nanofluids through heat exchangers. In this study, the pumping power of Cu-graphene water-based hybrid nanofluids was calculated using the equation available from the literature [33] as shown below by assuming a fixed mass flow rate (0.1 kg/s) and pressure drop (0.5×10^5 Pa).

$$\text{Pumping power} = \left(\frac{m}{\rho_{\text{hnf}}} \right) \times \Delta P \tag{10}$$

Figure 10 presents the variation of calculated pumping power of Cu-graphene hybrid nanofluids to the concentration of hybrid nanostructures at room temperature. From the figure, it can be seen that the pumping power decreases as the concentration of hybrid nanostructures increases. This could be possibly due to the increase in the density due to the increase in the hybrid nanostructure concentration and also because of the very low concentration of the hybrid nanostructures in water [52].

Heat transfer performance estimation using FOM analysis

Thermal performance of hybrid nanofluids is evaluated based on the figure of merit (FOM) analysis. FOM can be calculated using the ratio of the Mouromtseff number (Mo) of nanofluid and base fluid. Based on the value of FOM analysis, the suitability of nanofluids in different internal flow conditions can be judged and ranked. It is always desirable to have FOM greater than one to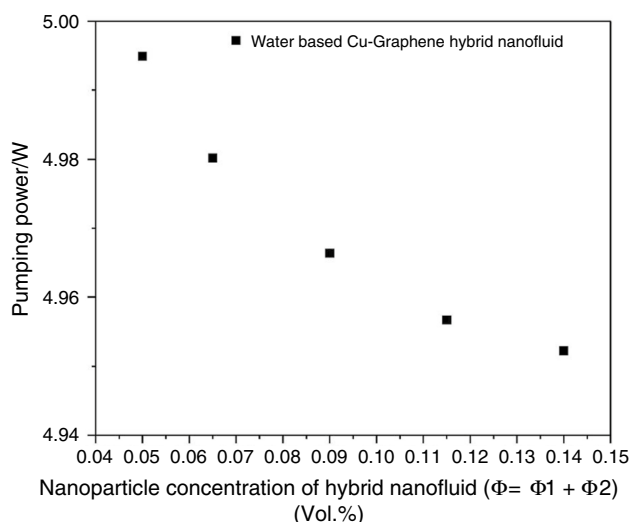 justify the use of nanofluids in laminar and turbulent flow conditions. FOM under laminar and turbulent flow conditions can be calculated as follows:

$$\text{FOM}_{\text{laminar}} = \frac{k_{\text{nf}}}{k_{\text{bf}}} = \frac{(\mu_{\text{nf}} - \mu_{\text{bf}})}{k_{\text{nf}} - k_{\text{bf}}} \tag{11}$$

$$\begin{aligned}
\text{FOM}_{\text{turbulent}} = \frac{M_{\text{onf}}}{M_{\text{obf}}} &= \left(\frac{k_{\text{nf}}}{k_{\text{bf}}} \right)^{0.6} \times \left(\frac{\rho_{\text{nf}}}{\rho_{\text{bf}}} \right)^{0.8} \\
&\times \left(\frac{c_{\text{pnf}}}{c_{\text{pbf}}} \right)^{0.4} \times \left(\frac{\mu_{\text{nf}}}{\mu_{\text{bf}}} \right)^{-0.47}
\end{aligned} \tag{12}$$

$$\text{where, } M_{\text{o}} = \left(\frac{\rho^{\text{a}} k^{\text{b}} C_{\text{p}}^{\text{d}}}{\mu^{\text{e}}} \right) 0 \tag{13}$$

In the above equations, $M_{\text{o,nf}}, M_{\text{o,bf}}, k_{\text{nf}}, k_{\text{bf}}, \rho_{\text{nf}}, \rho_{\text{bf}}, \mu_{\text{nf}}, \mu_{\text{bf}}, c_{\text{pnf}}$ and c_{pbf} indicate Mouromtseff number, thermal conductivity, density, dynamic viscosity, and specific heat of the hybrid nanofluid and base fluid, respectively, and $a = 0.8$, b = 0.6, d = 0.4, and $e = 0.47$ [25]. FOM of water-based Cu-graphene hybrid nanofluid was calculated under various internal flow conditions and shown in Fig. 11. From Fig. 11a and b, it is observed that the Cu-graphene hybrid nanofluids suit best under laminar flow conditions (FOM greater than 1) for showing better heat transfer capability. Also, it confirms that these hybrid nanofluids are not able to show better enhancement in their thermal performance under turbulent flow (internal flow) conditions due to their less-than-unity FOM value. FOM analysis helps researchers in reducing unsuccessful trial experiments.

A comparative table describing the comparison of present work with the studies existing in the literature is shown in
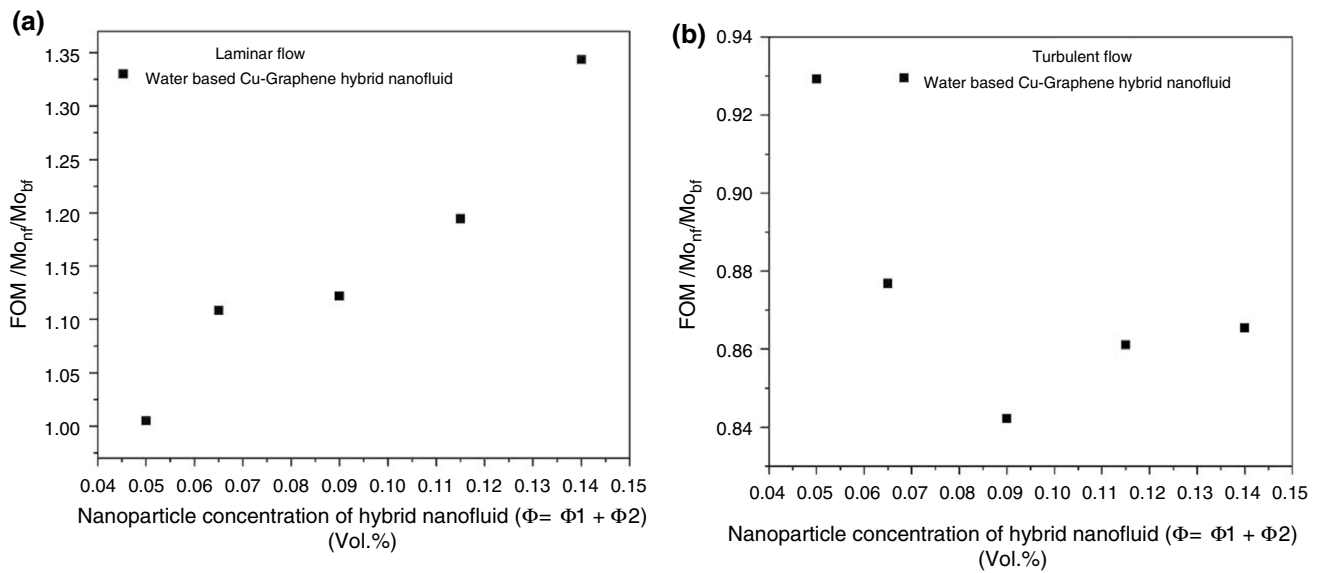
Fig. 11 FOM analysis of Cu-graphene hybrid nanofluids under (**a**) laminar and **b** turbulent flow conditions

Table 5 Table representing the comparison of current study with the existing literature

References	Type of nano-particle	Base fluid	Volume con-centration	Stabilizer	Enhancement in ther-mophysical properties / %		FOM analysis conducted (Yes/NO)	Suitable flow region
					Thermal conductiv-ity	Viscosity		
Mane et al. [25]	CuO -Fe$_3$O$_4$	Water	0.1 mass %	Chitosan	4.9	10	Yes	Laminar and turbulent
Kanti et al. [27]	Fly ash–Cu	Distilled water	0.5–4.0 vol.%	Triton X-100	13.1	45.18	Yes	Laminar and turbulent
Mostafizura et al. [30]	Al$_2$O$_3$– MWCNT	Radiator cool-ant	0.1–0.5 vol %	SDS	13.7	11	Yes	Laminar and turbulent
Samarshi et al. [31]	TiO$_2$	Water	10–100 ppm	PVP, Tween 20	8.3	50	Yes	Laminar
Huminic, G., & Huminic, A [53]	ND–Ni	Water	0.1, and 0.3 vol %	–	29.39	23.24	Yes	Laminar and turbulent
Farbod, M., & Rafati, Z. [54]	BN nanosheets	Ethylene glycol	0.5–2 vol %	Sodium cholate	24	–	Yes	Turbulent
Gómez-Vil-larejo et al. [55]	BNNTs	Dowtherm A	3.4, 5.8, and 8.6 vol %	Triton X-100	33	–	Yes	Laminar
Wang et al. [56]	Fe$_3$O$_4$	Water	0.1–3 vol%	–	90	130	Yes	Laminar and turbulent
Sundar et al. [57]	ND	propylene glycol/water mixture	0.2–1 vol %	–	18	1.66 times	Yes	Turbulent
Kumar, K. R., & Shaik, A. H. [58]	Cu-MXene	Water, Metha-nol, castor oil and silicon e oil	0.02–0.06 vol %	SDS	10 – 70	10 – 340	Yes	Laminar and turbulent (except for water based)
Present work	Cu-graphene	Water	0.05–0.14 vol %	–	35	65	Yes	Laminar

Table 5. From the table, it can be seen that the Cu-graphene hybrid nanofluids shows excellent stability against aggregation without using any surfactant and also exhibit considerable enhancement in the thermal conductivity and viscosity at very low concentration of hybrid nanostructures as compared to already reported works.

Uncertainty Analysis

To perform the uncertainty analysis, ASTM Performance Test Code PTC 19.8 was used [59]. For improving the measured data consistency and reliability, all the thermophysical parameters, i.e., thermal conductivity, density, and viscosity have been measured multiple times (minimum 3 times), and average data are stated along with their standard error value. The maximum percentage error data for thermal conductivity, density, and viscosity are 5%, 0.05%, and 1%, respectively. Since the specific heat and pumping power of nanofluid are calculated from the empirical equations (equation number), uncertainty analysis is not applicable for these properties/parameters.

Conclusions

Cu and graphene nanostructures required for preparing Cu-graphene hybrid nanofluids were produced using chemical reduction method and thermal treatment followed by grinding technique. The average particle size of Cu nanoparticles is found to be ~ 60 nm and graphene nanostructures represent a platelet/flake type structure as observed from FESEM analysis. Hybrid nanofluids are successfully prepared by dispersing the low concentration Cu and graphene nanostructures in water as the base fluid. These hybrid nanofluids exhibit exceptional stability against aggregation in water for at least 7 weeks.

Thermophysical properties of Cu-graphene hybrid nanofluids were successfully measured and calculated, indicating an enhancement in the thermal conductivity and viscosity of hybrid nanofluids at very low concentrations of nanostructures as compared to water. Moreover, the specific heat and pumping power of hybrid nanofluids were also effectively calculated using theoretical equations collected from the literature, and it was observed that the specific heat and pumping power decreased with an increase in the concentration of hybrid nanostructures in the base fluid. Experimental values of thermal conductivity and viscosity of Cu-graphene hybrid nanofluids are also validated with the existing theoretical equations from the literature. Finally, the thermal performance of heat exchanging devices under internal laminar and turbulent flow conditions is calculated by conducting the FOM analysis. FOM analysis suggested that the synthesized Cu-graphene hybrid nanofluids are suitable only under internal laminar flow conditions (as the value of FOM is greater than 1 in laminar flow).

Declarations

References

1. Xuan Z, Zhai Y, Li Y, Li Z, Wang H. Guideline for selecting appropriate mixing ratio of hybrid nanofluids in thermal management systems. Powder Technol. 2022;403:117425.
2. Jamei M, Karbasi M, Mosharaf-Dehkordi M, Olumegbon IA, Abualigah L, Said Z, Asadi A. Estimating the density of hybrid nanofluids for thermal energy application: application of non-parametric and evolutionary polynomial regression data-intelligent techniques. Measurement. 2022;189:110524.
3. Muneeshwaran M, Srinivasan G, Muthukumar P, Wang CC. Role of hybrid-nanofluid in heat transfer enhancement: a review. Int Commun Heat Mass Transfer. 2021;125:105341.
4. Said Z, Cakmak NK, Sharma P, Sundar LS, Inayat A, Keklikcioglu O, Li C. Synthesis, stability, density, viscosity of ethylene glycol-based ternary hybrid nanofluids: experimental investigations and model-prediction using modern machine learning techniques. Powder Technol. 2022;400:117190.
5. Tong Y, Boldoo T, Mr JH, Cho H. Improvement of photo-thermal energy conversion performance of MWCNT/Fe$_3$O$_4$ hybrid nanofluid compared to Fe$_3$O$_4$ nanofluid. Energy. 2020;196:117086.
6. Wang X, Wen Q, Yang J, Shittu S, Wang X, Zhao X, Wang Z. Heat transfer and flow characteristic of a flat confined loop thermosyphon with ternary hybrid nanofluids for electronic devices cooling. Appl Therm Eng. 2023;221:119758.
7. Alghamdi M, Fatima B, Hussain Z, Nisar Z, Alghamdi HA. Peristaltic pumping of hybrid nanofluids through an inclined asymmetric channel: a biomedical application. Mater Today Commun. 2023;35:105684.
8. Abdelkareem MA, Maghrabie HM, Abo-Khalil AG, Adhari OHK, Sayed ET, Radwan A, Olabi AG. Battery thermal

management systems based on nanofluids for electric vehicles. J Energy Storage. 2022;50:104385.

9. Struchalin PG, Kuzmenkov DM, Yunin VS, Wang X, He Y, Balakin BV. Hybrid nanofluid in a direct absorption solar collector: magnetite versus carbon nanotubes compete for thermal performance. Energies. 2022;15(5):1604.

10. Sanni SE, Olofin P, Okoro EE, Oni B, Okorie A. Ultrasonic thermophysical enhancement of a novel nanodoped vapour compression fluid for high cooling efficiency. Thermal Sci Eng Progress. 2022;36:101485.

11. Huminic G, Huminic A. Hybrid nanofluids for heat transfer applications: a state-of-the-art review. Int J Heat Mass Transf. 2018;125:82–103.

12. Bhatti MM, Abdelsalam SI. Scientific breakdown of a ferromagnetic nanofluid in hemodynamics: enhanced therapeutic approach. Math Modell Natural Phenom. 2022;17:44.

13. Abdelrazek AH, Alawi OA, Kazi SN, Yusoff N. Thermal performance evaluation for alumina coated MWCNTs composite nanofluid in annular passage of various eccentricities. Powder Technol. 2021;391:114–32.

14. Hussein OA, Rajab MH, Alawi OA, Falah MW, Abdelrazek AH, Ahmed W, Eltaweel M, Homod RZ, Yaseen ZM. Multiwalled carbon nanotubes-titanium dioxide nanocomposite for flat plate solar collectors applications. Appl Therm Eng. 2023;229:120545.

15. Yao Y, Sang D, Zou L, Wang Q, Liu C. A review on the properties and applications of WO_3 nanostructure-based optical and electronic devices. Nanomaterials. 2021;11(8):2136.

16. Abdelsalam SI, Alsharif AM, Abd Elmaboud Y, Abdellateef AI. Assorted kerosene-based nanofluid across a dual-zone vertical annulus with electroosmosis. Heliyon. 2023. https://doi.org/10.1016/j.heliyon.2023.e15916.

17. Tatar DK, Jha JM. Wet chemical synthesis and characterization of CuO nanoparticles and their application in pool boiling heat transfer. J Cryst Growth. 2023. https://doi.org/10.1016/j.jcrysgro.2023.127305.

18. Yang K, Wang J, Wu L, Yan Y, Tang X, Gan W, Li H. Controllable growth α-In2Se3 flakes by chemical vapor deposition. Res Phys. 2023. https://doi.org/10.1016/j.rinp.2023.106643.

19. Tu Y, Zhong J, Ding H, Zhang H, Lv G, Zhang J, Hou X. Preparation of fly ash supporting nano-TiO_2 composite photocatalyst by a wet mechanical grinding method. Chem Phys Lett. 2022;805:139978.

20. Chandan MR, Kumar KR, Shaik AH. Two-dimensional Cu nanostructures for efficient photo-catalytic degradation of methylene blue. Environ Sci: Adv. 2022;1(5):814–26.

21. Akgul G, Akgul FA. Impact of cobalt doping on structural and magnetic properties of zinc oxide nanocomposites synthesized by mechanical ball-milling method. Colloid and Interface Sci Commun. 2022;48:100611.

22. Suresh S, Venkitaraj KP, Selvakumar P, Chandrasekar M. Synthesis of Al_2O_3–Cu/water hybrid nanofluids using two step method and its thermo physical properties. Colloids Surf, A. 2011;388(1–3):41–8.

23. Abbasi SM, Rashidi A, Nemati A, Arzani K. The effect of functionalisation method on the stability and the thermal conductivity of nanofluid hybrids of carbon nanotubes/gamma alumina. Ceram Int. 2013;39(4):3885–91.

24. Tiwari AK, Pandya NS, Said Z, Chhatbar SH, Al-Turki YA, Patel AR. 3S (Sonication, surfactant, stability) impact on the viscosity of hybrid nanofluid with different base fluids: an experimental study. J Mol Liq. 2021;329:115455.

25. Mane NS, Tripathi S, Hemadri V. Effect of biopolymers on stability and properties of aqueous hybrid metal oxide nanofluids in thermal applications. Colloids Surf, A. 2022;643:128777.

26. Kanti P, Sharma KV, Khedkar RS, Rehman TU. Synthesis, characterization, stability, and thermal properties of graphene oxide based hybrid nanofluids for thermal applications: experimental approach. Diam Relat Mater. 2022;128:109265.

27. Kanti P, Sharma KV, Yashawantha KM, Jamei M, Said Z. Properties of water-based fly ash-copper hybrid nanofluid for solar energy applications: application of RBF model. Sol Energy Mater Sol Cells. 2022;234:111423.

28. Phanindra Y, Kumar SD, Pugazhendhi S. Experimental investigation on Al_2O_3 & Cu/Oil hybrid nano fluid using concentric tube heat exchanger. Mater Today: Proc. 2018;5(5):12142–50.

29. Kumar V, Sarkar J. Particle ratio optimization of Al_2O_3-MWCNT hybrid nanofluid in minichannel heat sink for best hydrothermal performance. Appl Therm Eng. 2020;165:114546.

30. Mostafizur RM, Rasul MG, Nabi MN, Saianand G. Properties of Al_2O_3-MWCNT/radiator coolant hybrid nanofluid for solar energy applications. Energy Rep. 2022;8:582–91.

31. Chakraborty S, Sarkar I, Behera DK, Pal SK, Chakraborty S. Experimental investigation on the effect of dispersant addition on thermal and rheological characteristics of TiO_2 nanofluid. Powder Technol. 2017;307:10–24.

32. Das S, Giri A, Samanta S, Kanagaraj S. Role of graphene nanofluids on heat transfer enhancement in thermosyphon. J Sci: Adv Mater Devices. 2019;4(1):163–9.

33. Elcioglu EB, Genc AM, Karadeniz ZH, Ezan MA, Turgut A. Nanofluid figure-of-merits to assess thermal efficiency of a flat plate solar collector. Energy Convers Manage. 2020;204:112292.

34. Chowdhury PP, Shaik AH, Chakraborty J. Preparation of stable sub 10 nm copper nanopowders redispersible in polar and nonpolar solvents. Colloids Surf, A. 2015;466:189–96.

35. Tran VQ, Doan HT, Nguyen NT, Do CV. Preparation of graphene nanoplatelets by thermal shock combined with ball milling methods for fabricating flame-retardant polymers. J Chem. 2019. https://doi.org/10.1155/2019/5284160.

36. Sharma V, Sundaramurthy A, Tiwari A, Sundramoorthy AK. Graphene nanoplatelets-silver nanorods-polymer based in-situ hybrid electrode for electroanalysis of dopamine and ascorbic acid in biological samples. Appl Surf Sci. 2018;449:558–66.

37. Shoghl SN, Jamali J, Moraveji MK. Electrical conductivity, viscosity, and density of different nanofluids: an experimental study. Exp Thermal Fluid Sci. 2016;74:339–46.

38. Yadav D, Nirala A, Kumar R, Singh PK. Density variation in nanofluids as a function of concentration and temperature. Mater Today: Proc. 2021;46:6576–80.

39. Balaji T, Rajendiran S, Selvam C, Lal DM. Enhanced heat transfer characteristics of water based hybrid nanofluids with graphene nanoplatelets and multi walled carbon nanotubes. Powder Technol. 2021;394:1141–57.

40. Wohld J, Beck J, Inman K, Palmer M, Cummings M, Fulmer R, Vafaei S. Hybrid nanofluid thermal conductivity and optimization: original approach and background. Nanomaterials. 2022;12(16):2847.

41. Maxwell JC. A treatise on electricity and magnetism. Vol 1. Clarendon press. (1873)

42. Hamilton RL, Crosser OK. Thermal conductivity of heterogeneous two-component systems. Ind Eng Chem Fundam. 1962;1(3):187–91.

43. Yu W, Choi SUS. The role of interfacial layers in the enhanced thermal conductivity of nanofluids: a renovated Maxwell model. J Nanopart Res. 2003;5:167–71.

44. Sahoo RR, Kumar V. Development of a new correlation to determine the viscosity of ternary hybrid nanofluid. Int Commun Heat Mass Transfer. 2020;111:104451.

45. Zhang H, Qing S, Gui Q, Zhang X, Zhang A. Effects of surface modification and surfactants on stability and thermophysical properties of TiO_2/water nanofluids. J Mol Liq. 2022;349:118098.

46. Pak BC, Cho YI. Hydrodynamic and heat transfer study of dispersed fluids with submicron metallic oxide particles. Exp Heat Transfer an Int J. 1998;11(2):151–70.

47. Brinkman HC. The viscosity of concentrated suspensions and solutions. J Chem Phys. 1952;20(4):571–571.

48. Einstein A . Investigations on the Theory of the Brownian Movement. Courier Corporation (1956)

49. Akilu S, Baheta AT, Sharma KV. Experimental measurements of thermal conductivity and viscosity of ethylene glycol-based hybrid nanofluid with TiO_2–CuO/C inclusions. J Mol Liq. 2017;246:396–405.

50. Chen H, Ding Y, He Y, Tan C. Rheological behaviour of ethylene glycol based titania nanofluids. Chem Phys Lett. 2007;444(4–6):333–7.

51. Batchelor GK. The effect of Brownian motion on the bulk stress in a suspension of spherical particles. J Fluid Mech. 1977;83(1):97–117.

52. Raj P, Subudhi S. A review of studies using nanofluids in flat-plate and direct absorption solar collectors. Renew Sustain Energy Rev. 2018;84:54–74.

53. Huminic G, Huminic A. Heat transfer capability of the hybrid nanofluids for heat transfer applications. J Mol Liq. 2018;272:857–70.

54. Farbod M, Rafati Z. Heat transfer, thermophysical and rheological behavior of highly stable few-layers of h-BN nanosheets/EG-based nanofluid. Mater Today Commun. 2022;33:104921.

55. Gómez-Villarejo R, Estellé P, Navas J. Boron nitride nanotubes-based nanofluids with enhanced thermal properties for use as heat transfer fluids in solar thermal applications. Sol Energy Mater Sol Cells. 2020;205:110266.

56. Wang H, Liang M, He Z, Kang X, Zhao Y, Zhao Y. Usefulness of adding magnetic nano-powders to water: introducing novel criteria for assessing heat transfer applications. Powder Technol. 2021;386:457–66.

57. Sundar LS, Singh MK, Sousa AC. Experimental thermal conductivity and viscosity of nanodiamond-based propylene glycol and water mixtures. Diam Relat Mater. 2016;69:49–60.

58. Kumar KR, Shaik AH. Synthesis, thermophysical characterization and thermal performance analysis of novel Cu-MXene hybrid nanofluids for efficient coolant applications. RSC Adv. 2023;13(42):29536–60.

59. Abernethy RB, Benedict RP, Dowdell RB. ASME measurement uncertainty (1985)